





RESEARCH ARTICLE

Nitroxyl (HNO) targets phospholamban cysteines 41 and 46 to enhance cardiac function

Gizem Keceli^{1,2} , Ananya Majumdar³, Chevon N. Thorpe⁴ , Seungho Jun², Carlo G. Tocchetti⁵ , Dong I. Lee², James E. Mahaney⁶, Nazareno Paolocci^{2,7}, and John P. Toscano¹ 

Nitroxyl (HNO) positively modulates myocardial function by accelerating Ca^{2+} reuptake into the sarcoplasmic reticulum (SR). HNO-induced enhancement of myocardial Ca^{2+} cycling and function is due to the modification of cysteines in the transmembrane domain of phospholamban (PLN), which results in activation of SR Ca^{2+} -ATPase (SERCA2a) by functionally uncoupling PLN from SERCA2a. However, which cysteines are modified by HNO, and whether HNO induces reversible disulfides or single cysteine sulfinamides (RS(O)NH_2) that are less easily reversed by reductants, remain to be determined. Using an ^{15}N -edited NMR method for sulfinamide detection, we first demonstrate that Cys46 and Cys41 are the main targets of HNO reactivity with PLN. Supporting this conclusion, mutation of PLN cysteines 46 and 41 to alanine reduces the HNO-induced enhancement of SERCA2a activity. Treatment of WT-PLN with HNO leads to sulfinamide formation when the HNO donor is in excess, whereas disulfide formation is expected to dominate when the HNO/thiol stoichiometry approaches a 1:1 ratio that is more similar to that anticipated in vivo under normal, physiological conditions. Thus, ^{15}N -edited NMR spectroscopy detects redox changes on thiols that are unique to HNO, greatly advancing the ability to detect HNO footprints in biological systems, while further differentiating HNO-induced post-translational modifications from those imparted by other reactive nitrogen or oxygen species. The present study confirms the potential of HNO as a signaling molecule in the cardiovascular system.

Introduction

Physiological levels of reactive oxygen and nitrogen species (ROS/RNS) participate in cellular signaling events by inducing chemical modifications of proteins that are discrete, site-specific, and reversible (Bachi et al., 2013). These target proteins, containing mostly very reactive thiols (i.e., cysteines), are transiently oxidized by ROS/RNS to enable transmission of the signal and then enzymatically reduced to their basal oxidation state by the glutathione and thioredoxin systems. Increasingly, this “redox regulation” is emerging as an important means by which ROS/RNS modulate basal myocardial function. Yet the identification within the myocardium of specific thiol residues whose selective and reversible chemical modifications by ROS/RNS contribute to enhance myocardial mechanical performance remains far from being complete (Tocchetti et al., 2011; Gao et al., 2012). This knowledge gap stems in part from the still limited number of methodologies available to identify these residues and their modifications.

Nitroxyl (azanone, HNO) is the one-electron reduced sibling of nitric oxide (NO ; Feelisch, 2003; Kemp-Harper, 2011). HNO

donors enhance cardiac contractility and accelerate relaxation in both normal and failing hearts (Paolocci et al., 2001, 2003, 2007; Tocchetti et al., 2011). Central to HNO’s positive modulation of cardiac function is its ability to augment Ca^{2+} cycling at the level of the SR. After cardiac muscle excitation, the opening of voltage-dependent L-type Ca^{2+} channels allows the entry of a small amount of Ca^{2+} that in turn stimulates a greater release of Ca^{2+} from the RYRs (RYR2) to trigger contraction at the myofilament level (Bers, 2002). During cardiac relaxation, Ca^{2+} must reaccumulate into the SR, a process largely driven by SERCA2a activity (Bers, 2002), with some Ca^{2+} extrusion occurring via sarcolemmal $\text{Na}^+/\text{Ca}^{2+}$ exchanger (Bers, 2002).

Phospholamban (PLN) is a key determinant of SERCA2a activity and thus cardiac SR Ca^{2+} cycling. When dephosphorylated, PLN functionally couples with SERCA2a, inhibiting SR Ca^{2+} reuptake. Conversely, upon phosphorylation by $\beta\text{AR}/\text{PKA}$, the PLN brake on SERCA2a is removed, resulting in enhanced SR Ca^{2+} pump activity (Hagemann and Xiao, 2002; Li et al., 2003; MacLennan and Kranias, 2003; James et al., 2012). The impact of

¹Department of Chemistry, Johns Hopkins University, Baltimore, MD; ²Division of Cardiology, Johns Hopkins School of Medicine, Baltimore, MD; ³Biomolecular NMR Center, Johns Hopkins University, Baltimore, MD; ⁴Department of Biochemistry, Virginia Polytechnic Institute and State University, Blacksburg, VA; ⁵University of Naples “Federico II”, Naples, Italy; ⁶Edward Via College of Osteopathic Medicine, Blacksburg, VA; ⁷Department of Biomedical Sciences, University of Padova, Padova, Italy.

Correspondence to John P. Toscano: jtoscano@jhu.edu.

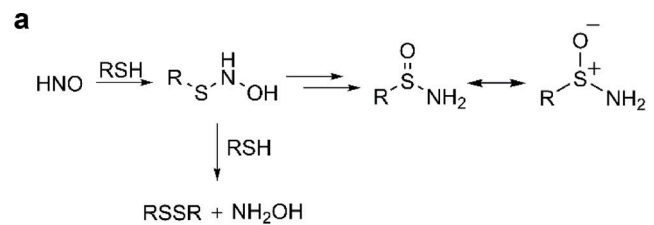
© 2019 Keceli et al. This article is distributed under the terms of an Attribution–Noncommercial–Share Alike–No Mirror Sites license for the first six months after the publication date (see <http://www.rupress.org/terms/>). After six months it is available under a Creative Commons License (Attribution–Noncommercial–Share Alike 4.0 International license, as described at <https://creativecommons.org/licenses/by-nc-sa/4.0/>).

HNO on PLN is similar to that of PKA phosphorylation, i.e., PLN functional uncoupling from SERCA2a; however, HNO actions are not PKA dependent, but rather due to redox-mediated PLN oligomerization (Sivakumaran et al., 2013). In fact, enhancement of SERCA2a activity by HNO, and thus its inotropic and lusitropic effects, originate at least in part from modifications of the three cysteine residues present in the PLN transmembrane domain, namely Cys36, Cys41, and Cys46. When these residues are all mutated to alanines, or preblocked (by alkylating agents; Froehlich et al., 2008; Sivakumaran et al., 2013), the HNO-induced increase in SERCA2a catalytic efficiency is lost.

At a molecular level, in the SR membrane or in SDS gels, PLN exists as an equilibrium mixture of a homopentamer and a monomer (Wegener and Jones, 1984; Jones et al., 1985). Although the PLN monomer has been long considered as the SERCA2a inhibitory species, recent reports indicate that SERCA interacts with the PLN pentamer, too, pointing to a potential role of the latter in regulating SERCA activity (Kimura et al., 1997; Stokes et al., 2006; Glaves et al., 2011; Smeazzetto et al., 2013; Vostrikov et al., 2013). Based on site-directed mutagenesis studies, the PLN homopentamer is stabilized by hydrophobic interactions. We previously reported that HNO affects PLN oligomerization or conformation in a redox-dependent manner; the thiol-reducing agent dithiothreitol (DTT) reverses HNO-induced formation of PLN oligomerization (Froehlich et al., 2008; Sivakumaran et al., 2013). Yet the specific identities of PLN transmembrane cysteines involved in the HNO-induced PLN oligomerization remain unclear. Equally important, the nature of HNO-imparted modifications of these residues, i.e., reversible versus irreversible, needs to be fully resolved, because HNO donors are currently in clinical trials to evaluate the safety and efficacy in patients with acute decompensated heart failure (Sabbah et al., 2013).

In solution-phase studies, HNO interacts with thiols to form an *N*-hydroxysulfenamide intermediate (RSNHOH), which is then converted into a disulfide or a sulfinamide (RS(O)NH₂) depending on the relative concentration of thiol, or in the atypical case of C-terminal cysteines, a sulfenic acid (Doyle et al., 1988; Wong et al., 1998; Keceli and Toscano, 2014). When thiols are in excess, the end product is typically a disulfide, whereas at low thiol concentrations, the end product is a sulfinamide (Fig. 1 a).

Recent evidence indicates that HNO-derived sulfinamides can also be reduced back to free thiols in the presence of excess thiol, although this reaction is significantly slower than the reduction of disulfides (Keceli and Toscano, 2012; Keceli et al., 2013). When a biological system such as that involving cardiac PLN cysteines is being studied, it remains to be determined whether HNO induces an intermolecular disulfide, an intramolecular disulfide, and/or a sulfinamide (Fig. 1 b). Based on HNO's specificity and reversibility of action in a biological system that may depend on levels of bioavailable thiols, HNO's potential signaling capacity *in vivo* can be tested. However, addressing this question has been hampered so far by the limited number of tools available to detect HNO-modified thiol residues in proteins as well as the extreme difficulties encountered so far in the application of mass spectrometry



R = alkyl or aryl group of a small molecule, peptide, or protein

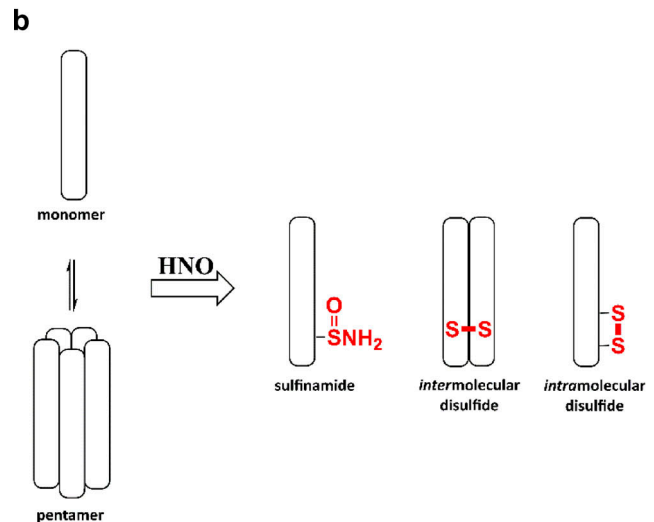


Figure 1. **HNO-induced cysteine modifications.** (a) The reaction of HNO with thiols. (b) Potential HNO-induced modifications of PLN: inter- or intramolecular disulfide and/or sulfinamide formation.

techniques to the study of PLN (Donzelli et al., 2006; Hoffman et al., 2009).

Solution and solid-state NMR techniques have been used to investigate the structural topology and dynamics of monomeric and pentameric PLN, its interaction with lipids, its regulation of SERCA, and the impact of PLN phosphorylation in a lipid bilayer, detergent micelles, and organic solvents (Lamberth et al., 2000; Zamoon et al., 2003; Oxenoid and Chou, 2005; Abu-Baker and Lorigan, 2006; Traaseth et al., 2008, 2009; Veglia et al., 2010; Verardi et al., 2011). A well-known approach is the use of ¹⁵N uniformly- or selectively-labeled PLN (Veglia et al., 2010). In addition, ¹⁵N-edited NMR spectroscopy has allowed the detection of HNO-derived sulfinamides in several systems including small molecules, peptides, and proteins (Keceli et al., 2013). This approach has not yet been used to evaluate HNO-induced modifications on PLN transmembrane cysteines.

Hence, with this tool in hand, and also using SERCA2a activity assays in the presence of WT-PLN and its single cysteine mutants expressed in High Five cells (Waggoner et al., 2004), we are pleased to report herein investigations to identify the specific cysteine(s) that upon modification by HNO lead to enhanced SERCA2a activity and to determine which chemical modification prevails, i.e., sulfinamide versus intramolecular or intermolecular disulfide bond formation when the HNO:thiol

ratio approaches values similar to those expected in in vivo cardiac cells.

Materials and methods

Materials

HPLC and mass spectrometry-grade acetonitrile (ACN), and a bicinchoninic acid assay kit were purchased from Thermo Fisher Scientific. DMSO- d_6 , D_2O , and ^{15}N -labeled hydroxylamine hydrochloride were purchased from Cambridge Isotope Laboratories. DTT, β -mercaptoethanol, and 7-diethylamino-3-(4-maleimidophenyl)-4-methylcoumarin (CPM) were of the highest purity available and obtained from Sigma-Aldrich. The syntheses of the HNO donor, Angeli's salt ($Na_2N_2O_3$, AS) and ^{15}N -labeled Angeli's salt (^{15}N -AS), were performed as previously described (Bonner and Ravid, 1975; Hughes and Cammack, 1999). The HNO donor, 2-methylsulfonyl benzene *N*-hydroxy sulfonamide (2-methylsulfonyl Pilot's acid, 2-MSPA; Toscano et al., 2011; Sabbah et al., 2013; Zhu et al., 2015), the ^{15}N -labeled HNO donor, 2-methylsulfonyl benzene ^{15}N -hydroxy sulfonamide (^{15}N -2-MSPA; Toscano et al., 2011; Sabbah et al., 2013; Zhu et al., 2015), and the donor byproduct, 2-(methylsulfonyl)benzenesulfonic acid (2-MSSA), were gifts from CardioXyl Pharmaceuticals. Dodecylphosphocholine (DPC) was purchased from Avanti Polar Lipids. Milli Q water was used for all purifications and experiments.

Peptide synthesis, purification, and reconstitution

WT-PLN and its single cysteine-containing (C41,46A-PLN, C36,46A-PLN, C36,41A-PLN) or two cysteine-containing variants (C36A-PLN and C46A-PLN) were synthesized on a Symphony Quartet peptide synthesizer (Protein Technologies) and purified by HPLC (Agilent HPLC equipped with a 1200 quaternary pump system and diode array detector) on a C4 polymer-supported reverse-phase column following literature procedures (Karim et al., 2000; Lockwood et al., 2003; Abu-Baker and Lorigan, 2006). In all cases, the identity of PLN and its variants were confirmed by MALDI-MS (Bruker AutoFlex III MALDI-TOF/TOF Mass Spectrometer equipped with a 355-nm pulsed UV laser and operated in the positive ionization mode) as described in the literature (Karim et al., 2000; Lockwood et al., 2003). The purified product was quantified based on a bicinchoninic acid assay (Smith et al., 1985). Proteins were stored at $-80^{\circ}C$ in lyophilized form until use. The proteins were reconstituted using 9 mM DPC in 10 mM sodium phosphate buffer with 50 μM of the metal chelator, diethylenetriamine pentaacetic acid, at pH 7.4 to have a final concentration of 0.5 or 60 μM PLN (Veglia et al., 2010). Following reconstitution, the α -helical structure of the samples were confirmed on an Aviv Circular Dichroism Spectrometer (Online supplemental figures).

Incubation of WT-PLN and its variants with HNO

The incubations were performed as previously described (Keceli and Toscano, 2012; Keceli et al., 2013). Stock solutions of AS were prepared in 0.01 M NaOH, kept on ice, and used within 15 min of preparation. Stock solutions of 2-MSPA and ^{15}N -2-MSPA were prepared in ACN and used within 15 min of

preparation. Stock solutions of the donor byproducts, NO_2^- and 2-MSSA, were dissolved in 0.01 M NaOH and ACN/ H_2O (1:1, vol/vol), respectively. WT-PLN and its variants (0.5 or 60 μM) reconstituted in pH 7.4 buffer were incubated with various concentrations of AS, 2-MSPA, or ^{15}N -2-MSPA (as indicated) at $37^{\circ}C$ for 30 min in a block heater. In all cases, the final volume of ACN did not exceed 1% of the total volume. As controls, incubations were also performed with donor byproducts NO_2^- and 2-MSSA under the same conditions. For some experiments, HNO-treated PLN samples were incubated further in the presence of 50 mM DTT or β -mercaptoethanol (as indicated) at $37^{\circ}C$ for 26 h. The samples were then prepared for either electrophoresis or NMR analysis.

For NMR analysis, the samples were flash frozen and lyophilized. Following lyophilization, the samples were redissolved in DMSO- d_6 for NMR analysis as described previously (Keceli et al., 2013). For electrophoresis and immunoblotting, the samples were diluted with sample loading buffer and analyzed immediately.

NMR analyses

All NMR analyses were conducted on a Bruker Avance II 600 MHz (1H) NMR spectrometer equipped with a cryogenically cooled probe. 1H NMR and ^{15}N -edited 1H one-dimensional (1-D) and two-dimensional (2-D) NMR analyses were performed in DMSO- d_6 at 298 K. ^{15}N -edited 1H 1D- and 2D-NMR spectra were acquired using the heteronuclear single quantum correlation (HSQC) pulse sequence for selectively identifying ^{15}N -labeled sites in the protein. Chemical shifts are reported in parts per million relative to residual DMSO (2.49 ppm for 1H). In all NMR experiments involving the detection of sulfonamide on PLN, ^{15}N -labeled benzamide was added as an internal standard immediately before NMR analysis. The samples were normalized with respect to the internal standard for comparison as described previously (Keceli et al., 2013). In these NMR experiments, we observe both the SD and SEM in sulfonamide detection to be less than or equal to $\pm 5\%$ (Keceli et al., 2013).

Electrophoresis and immunoblotting

WT-PLN and its variants were analyzed by electrophoresis and immunoblotting as previously described (Froehlich et al., 2008). Briefly, SDS-PAGE using 15% polyacrylamide was performed using standard procedures (Laemmli, 1970). Samples were either loaded directly or boiled for 5 min before loading. Upon separation by gel electrophoresis, the proteins were transferred via Western blotting onto polyvinylidene difluoride membrane (Bio-Rad). After blocking the membrane with 1% nonfat dry milk for 1 h, it was incubated overnight at $4^{\circ}C$ with anti-PLN monoclonal antibody (2D12; Affinity Bioreagents). The membrane was washed and incubated for 1 h with horseradish peroxidase-conjugated anti-mouse IgG secondary antibody (Upstate Cell Signaling Solutions). After washing, the chemiluminescent signals were generated by treating the membrane with enhanced chemiluminescence reagents (ECL Western blotting substrate; Pierce) and captured on film. PLN bands (monomer, dimer, and pentamer) were assigned based on a standard molecular weight marker (Bio-Rad). All gels and Western blots were run using a

Bio-Rad Mini-Protein II electrophoresis and Western blotting system.

PLN mutagenesis

Single cysteine PLN constructs were made using the null-cysteine canine PLN complementary DNA, which had all three native cysteine residues modified to alanine (C36A, C41A, C46A), as described (Froehlich et al., 2008). The QuikChange II XL site-directed mutagenesis kit (Stratagene) was used to reintroduce a cysteine residue individually at each native position. DNA sequencing was used to verify the correct PLN sequence for each mutant. The mutant complementary DNAs were individually incorporated into a recombinant baculovirus construct that was purified, amplified, and used to express the PLN species for these experiments, as reported previously (Waggoner et al., 2004).

Cardiomyocyte isolation

Cardiomyocytes were isolated as described (Sivakumaran et al., 2013). Hearts from male (2–6 months old) WT (C57BL/6) mice were quickly removed from the chest, and the aorta was retrogradely perfused at constant pressure (100 cm H₂O) at 37°C for 3 min with a Ca²⁺-free bicarbonate-based isolation buffer containing (in mM) 120 NaCl, 5.4 KCl, 1.2 NaH₂PO₄, 20 NaHCO₃, 1.6 MgCl₂, 5.5 glucose, 2,3-butanedione monoxime (1 mg/ml), and taurine (0.628 mg/ml), gassed with 95% O₂/5% CO₂. The enzymatic digestion was initiated by adding 1.2 mg/ml collagenase type 2 (Worthington Biochemical) and 40 µg/ml protease type XIV (Sigma-Aldrich) to the perfusion solution. After ~10 min, the heart was removed and cut into several chunks in the same enzyme solution. This solution containing dispersed myocytes was filtered through a 150-µm mesh and gently centrifuged at 800 rpm for 1 min.

Activity assays

All coexpressed samples used for activity studies comprise a SERCA2a/PLN mole ratio of 1:1.6, where SERCA2a is under full-regulatory control of PLN. [AS/HNO]-dependent activation of SERCA2a ATPase activity was measured colorimetrically using the malachite green-ammonium molybdate assay (Lanzetta et al., 1979). High Five microsomes containing SERCA2a ± PLN were pretreated with the HNO donor, AS (100 µM), and were incubated at room temperature for 10 min. The protein treated with the desired level of AS was suspended (0.05 mg/ml total protein, 13.6 nM SERCA2a, and 21.2 nM PLN) in 50 mM MOPS, 3 mM MgCl₂, 100 mM KCl, 1 mM EGTA, and 0–1.0 mM CaCl₂, pH 7.0, to give a range of [Ca²⁺] (Autry and Jones, 1997). To initiate the ATPase reaction, 5 mM MgATP was added to the incubation tubes at 37°C, and phosphate (P_i) liberation was monitored over a 10-min period. Samples were pretreated with 20 µg of Ca²⁺ ionophore A23187/mg of total protein to prevent Ca²⁺ buildup within the microsomes during the assay.

To determine SERCA2a ATPase activity in cardiomyocytes, freshly isolated cells were resuspended in the Ca²⁺-free assay buffer to have a final concentration of 0.5 mg/ml total protein. The samples were incubated in the presence or absence of 5 µM CPM for 15 min at room temperature to block cysteine residues

(Liu and Pessah, 1994; Feng et al., 1999). Following treatment with the HNO donor, AS (100 µM), for 20 min at room temperature, the samples were immediately analyzed by malachite green-ammonium molybdate assay at 0 or 1 µM [Ca²⁺]_{free}. In all cases, control samples were exposed to the same experimental conditions in the presence of the vehicle. Comparisons were performed using one-way ANOVA followed by Student-Newman-Keuls multiple comparison test.

Assessment of sarcomere shortening in isolated murine myocytes

Following cardiomyocyte isolation from WT mice, the cell pellet was promptly resuspended in isolation buffer added with 125 µM Ca²⁺ and bovine serum albumin (5 mg/ml). After myocyte separation by gravity (10 min), the supernatant was aspirated and myocytes were resuspended in Tyrode's solution (in mM: 140 NaCl, 10 HEPES, 1 MgCl₂, 5 KCl, 5.5 glucose, adjusted to pH 7.4) supplemented with 250 µM Ca²⁺. The final cell pellet was suspended in 1 mM Ca²⁺.

Sarcomere shortening was measured as described (Sivakumaran et al., 2013). Briefly, the cells were field stimulated continuously for 10–15 min to establish contractile stability at the start of each experiment. Recording of twitch amplitude started during the stabilization period and cell shortening data were collected through the whole experiment. Cells were imaged using field stimulation (Warner Instruments) in an inverted fluorescence microscope. Sarcomere length was measured by real-time Fourier transform. The cells were superfused with Tyrode's solution, and the test solutions were rapidly switched. Stable cells were used to examine the effects of all the interventions on myocyte contractility (each in separate groups of cells). The interventions tested were CPM (20 nM) and AS/HNO (500 µM) or isoproterenol (ISO; 10 nM) in the presence or absence of prior CPM (20 nM) treatment. In all cases, the cells were superfused with the indicated test solution for 10 min with a flow rate of 1.5 ml/min. The statistical significance of the differences between treatments for studies using myocytes from WT mice was evaluated by one-way ANOVA using Tukey's multiple comparison test and/or paired *t* test.

Online supplemental material

Figs. S1 and S2 show circular dichroism (CD) spectra of WT-PLN and its variants. Fig. S3 gives the ¹⁵N-edited ¹H 1D-NMR spectrum of C36,46A-PLN treated with ¹⁵NH₂OH. Figs. S4–S7 show SDS-PAGE analyses of WT-PLN and its single cysteine variants treated with various concentrations of HNO donor.

Results

PLN Cys41 and Cys46 are the main targets of HNO based on ¹⁵N-edited NMR spectroscopy

PLN has three cysteine residues (Cys36, Cys41, and Cys46), all located in the transmembrane domain (Simmerman et al., 1986; Fujii et al., 1987). As per our previous studies, HNO modifies one or more of these residues to functionally uncouple PLN from SERCA2a (Froehlich et al., 2008; Sivakumaran et al., 2013), but the chemical nature of the HNO-induced modifications,

i.e., sulfinamide versus disulfides, and exact cysteine residue(s) involved remain unclear. Using several peptides and proteins, we have recently shown that the use of a thiol-to-HNO donor ratio of 1:5 or 1:10 under physiological conditions results mainly in the formation of the corresponding sulfinamides (Keceli and Toscano, 2012; Keceli et al., 2013). In addition, higher sulfinamide yields were obtained with cysteines adjacent to a leucine residue (VYPCLA) compared with those adjacent to a glycine residue (VYPGCA), presumably due to steric hindrance of the disulfide-forming reaction (Keceli and Toscano, 2012). Considering that PLN cysteine residues are located in the isoleucine/leucine zipper of PLN ($F^{36}CLILI^{41}CLLLI^{46}CII$; Simmerman et al., 1986; Fujii et al., 1987), we directly tested whether exposure of PLN thiols to HNO leads to the formation of the corresponding sulfinamides. To answer this important question, single cysteine variants of PLN (C41,46A-PLN, C36,46A-PLN, and C36,41A-PLN) were treated with the $H^{15}NO$ donor, ^{15}N -2-MSPA (Toscano et al., 2011; Sabbah et al., 2013; Zhu et al., 2015), which decomposes to produce HNO with a half-life of 2 min under physiologically relevant conditions (Sabbah et al., 2013). The samples were then analyzed with an ^{15}N -edited NMR method for sulfinamide detection (Keceli et al., 2013). This method provides simplified NMR spectra via application of an isotope filter for ^{15}N to detect protons bonded to the ^{15}N nuclei selectively (Breeze, 2000; Donzelli et al., 2006; Keceli et al., 2013). These investigations have demonstrated that the characteristic NMR region for sulfinamide detection is 5.0–6.5 ppm (Keceli et al., 2013). Sulfinamide peaks are observed upon treatment of C36,46A-PLN (single Cys at position 41) and C36,41A-PLN (single Cys at position 46) with excess $H^{15}NO$; however, no sulfinamide modification is detected on C41,46A-PLN (single Cys at position 36; Fig. 2, a–g). In all cases, the sulfinamide ^{15}NH peaks appear at ~ 5.94 ppm in the 1H dimension, and at ~ 88 and ~ 89 ppm in the ^{15}N dimension. It should be noted that the presence of two sulfinamide peaks in the 2D-NMR spectra (Fig. 2, b–d) is attributed to the generation of sulfinamide diastereomers (Keceli et al., 2013). When the interaction of HNO with thiols results in disulfide formation, $^{15}NH_2OH$ is expected to be released as a byproduct (Fig. 1a). As a control, we have treated PLN with $^{15}NH_2OH$ to test whether, although unlikely, these two species react to generate a species with an NMR peak, which could be misinterpreted as the presence of a PLN sulfinamide. Control experiments following $^{15}NH_2OH$ treatment of C36,46A-PLN did not produce any peaks in the characteristic sulfinamide region (Online supplemental figures).

Although significant disulfide bond formation is not expected at these thiol-to-HNO donor ratios, the presence of intermolecular disulfide bonds between PLN single cysteine variants was tested by electrophoresis and immunoblotting. The lack of HNO-induced PLN dimer upon treatment of these variants with varying concentrations of HNO donor (0–10 mM) supports that sulfinamide formation is the only HNO-derived modification under these conditions (Online supplemental figures). Moreover, the observed decrease in the pentamer band is consistent with the previously reported destabilization of PLN pentamer following modification of cysteine residues (Fujii et al., 1989; Karim et al., 1998). Overall, these results point

to the more reactive nature of PLN cysteine residues 41 and 46 toward HNO.

Comparison of sulfinamide yields in the presence of an internal standard indicates that more sulfinamide is formed on C36,41A-PLN compared with C36,46A-PLN (Fig. 2, e–g). Since the presence of more than one cysteine residue might affect the end products (i.e., sulfinamide vs. disulfide), we also employed the double cysteine variants, C36A-PLN and C46A-PLN. As expected, treatment of these PLN variants with the $H^{15}NO$ -donor results in the detection of sulfinamide peaks for both variants at ~ 5.95 ppm (Fig. 2, h, i, l, and m). Although it was not possible to distinguish among the sulfinamides on different cysteine residues, the total amount of sulfinamide detected in the presence of an internal standard was compared.

Consistent with our results with the single cysteine PLN variants, significantly more sulfinamide is observed on C36A-PLN (Cys at positions 41 and 46) compared with C46A-PLN (Cys at positions 36 and 41) (Fig. 2, l and m). These findings further support the more reactive nature of cysteines 46 and 41 toward HNO, with Cys46 being the most reactive.

A high HNO/thiol ratio leads to sulfinamide formation on Cys46 and Cys41

Our previous studies with WT-PLN have pointed to the formation of disulfide bonds, potentially both intramolecular and intermolecular, upon exposure to HNO (Froehlich et al., 2008; Sivakumaran et al., 2013). Furthermore, the intermolecular disulfide linkage between PLN monomers, resulting in the observation of PLN dimer, was proposed to take place in the pentameric species (Froehlich et al., 2008; Sivakumaran et al., 2013). The generation of an intermolecular disulfide bond between individual C36A-PLNs (and also C46A-PLNs) is not expected due to the lack of stable pentameric species in these samples under our experimental conditions (data not shown). However, the formation of an intramolecular disulfide bond might be feasible between cysteines 41 and 46 in C36A-PLN (Wouters et al., 2007, 2010; Froehlich et al., 2008). To determine the potential presence of disulfide bonds, the total amount of sulfinamide in C36A-PLN was compared with the sum of the amounts of sulfinamides in C36,46A-PLN and C36,41A-PLN upon treatment with excess HNO. These NMR analyses show comparable amounts of sulfinamides. If a potential disulfide bond were formed in C36A-PLN under these conditions, then the total amount of sulfinamide observed should have been significantly less than the sum of sulfinamides detected on Cys41 of C36,46A-PLN and Cys46 of C36,41A-PLN. Identical analyses conducted with C46A-PLN (Cys at positions 36 and 41) provided similar results. These findings point to the lack of significant amount of HNO-derived disulfide bonds in C36A-PLN and C46A-PLN under these conditions, thus making sulfinamide formation the major modification upon exposure of these PLN variants to excess HNO.

To gain additional insight into the HNO-derived modifications in WT-PLN, we probed these samples for sulfinamide modification. As seen in Fig. 2 j and Fig. 2 n, sulfinamide peaks are detected (at ~ 5.94 ppm) upon treatment of WT-PLN with excess HNO. To the best of our knowledge, this is the first time a

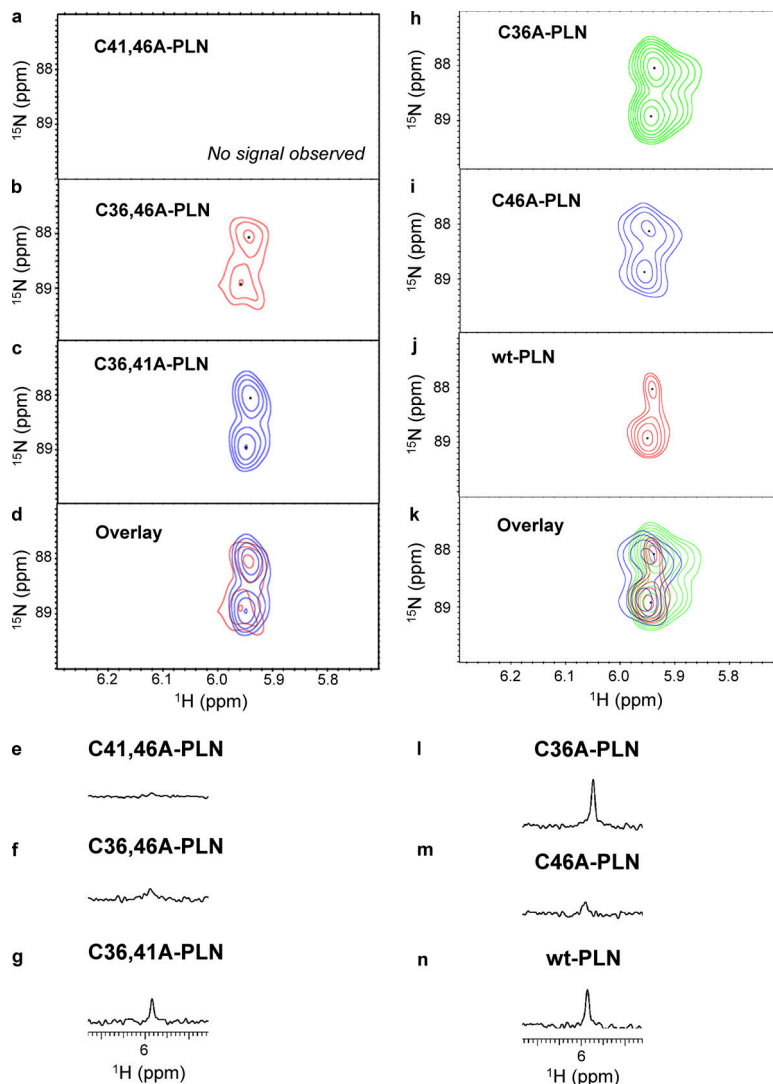


Figure 2. Sulfinamide signals on WT-PLN and its variants. (a–c) Selected region of ^{15}N -edited ^1H 2D-NMR spectra showing C41,46A-PLN (a; 60 μM , single Cys at position 36), C36,46A-PLN (b; 60 μM , single Cys at position 41; red), and C36,41A-PLN (c; 60 μM , single Cys at position 46; blue) upon treatment with the H^{15}NO donor, ^{15}N -2-MSPA (1 mM) in phosphate buffer containing DPC (pH 7.4) at 37°C for 30 min. (d) Overlay of H^{15}NO -derived sulfinamide signals. (e–g) Selected region of ^{15}N -edited ^1H 1D-NMR spectra showing C41,46A-PLN (e; 60 μM , single Cys at position 36), C36,46A-PLN (f; 60 μM , single Cys at position 41), and C36,41A-PLN (g; 60 μM , single Cys at position 46) upon treatment with the H^{15}NO donor, ^{15}N -2-MSPA (1 mM) in phosphate buffer containing DPC (pH 7.4) at 37°C for 30 min. (h–j) Selected region of ^{15}N -edited ^1H 2D-NMR spectra showing C36A-PLN (h; 60 μM , Cys at positions 41 and 46; green), C46A-PLN (i; 60 μM , Cys at positions 36 and 41; blue), and WT-PLN (j; 60 μM ; red) upon treatment with the H^{15}NO donor, ^{15}N -2-MSPA (1 mM) in phosphate buffer containing DPC (pH 7.4) at 37°C for 30 min. (k) Overlay of H^{15}NO -derived sulfinamide signals. (l–n) Selected region of ^{15}N -edited ^1H 1D-NMR spectra showing C36A-PLN (l; 60 μM , Cys at positions 41 and 46), C46A-PLN (m; 60 μM , Cys at positions 36 and 41), and WT-PLN (n; 60 μM) upon treatment with the H^{15}NO donor, ^{15}N -2-MSPA (1 mM) in phosphate buffer containing DPC (pH 7.4) at 37°C for 30 min.

sulfinamide modification has been observed on WT-PLN. Moreover, the amount of sulfinamide detected is more than that observed for C46A-PLN, and similar to that of C36A-PLN (Fig. 2, l–n). The weaker signal observed for WT-PLN in the 2D-NMR spectrum (Fig. 2j) is presumably due to precipitation of WT-PLN during prolonged data collection. Consistent with this observation, a diluted sample of WT-PLN produced stronger sulfinamide signals compared with the concentrated sample during 2D-NMR analysis (data not shown). Overall, these results are in agreement with cysteines 46 and 41 being the main sites of HNO reactivity with PLN.

Modification of PLN transmembrane cysteines at low HNO /thiol ratio

High ratios of HNO donor to thiol are easy to obtain in vitro, but unlikely to occur in vivo. Therefore, in order to mimic more physiologically relevant conditions, we repeated the experiments reported above in the presence of lower concentrations of HNO donors. Treatment of WT-PLN with a comparable amount of HNO donor caused a significant ($\sim 87\%$) decrease in sulfinamide formation (Fig. 3, a and b) relative to the experiments

described above. To test if this observation was due to the lack of reactivity between PLN thiols and HNO at these lower HNO concentrations, C36,41A-PLN was treated with HNO under the same conditions. No decrease in sulfinamide formation was observed in this variant (Fig. 4, a and b), indicating that Cys46 is able to trap HNO to the same extent under both conditions. Although the amount of sulfinamide detected on C36,46A-PLN was markedly affected at low HNO concentrations, it does not account for the observed decrease in the total amount of sulfinamide on WT-PLN (Fig. 5, a and b).

Based on the known reactivity of HNO with thiols (Doyle et al., 1988; Wong et al., 1998), an obvious explanation is the generation of intermolecular or intramolecular disulfide linkages (Froehlich et al., 2008; Sivakumaran et al., 2013; Fig. 1, a and b). Analysis of WT-PLN samples by electrophoresis and immunoblotting demonstrated the HNO -derived dimer formation, consistent with our previous findings (Online supplemental figures; Froehlich et al., 2008). However, treatment of WT-PLN samples with approximately equimolar quantities of HNO donor did not produce significant amounts of PLN dimer (data not shown). Hence intermolecular disulfide bonds are not

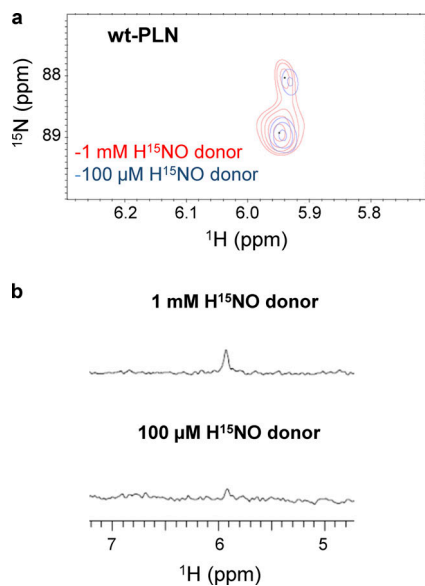


Figure 3. **Sulfinamide formation on WT-PLN at different concentrations of HNO donor.** (a and b) Comparison of the sulfinamide signals generated on WT-PLN (60 μ M) upon treatment with 1 mM (red) or 100 μ M (blue) 15 N-2-MSPA by 15 N-edited 1 H 2D-NMR (a) and 15 N-edited 1 H 1D-NMR analysis (b).

the major contributors under these conditions, and an intramolecular disulfide bond may play a role.

The involvement of disulfide modifications was investigated further by using C36A-PLN. Lowering the relative concentration of HNO donor resulted in a marked decrease ($\sim 80\%$) in sulfinamide yield as expected (Fig. 6, a and b). In agreement with the WT-PLN data, these findings support the formation of a potential intramolecular disulfide linkage. Although similar results were obtained with C46A-PLN (Fig. 6, c and d), the possible inefficient trapping of HNO by Cys41 at these concentrations, as observed with C36,46A-PLN (Fig. 5), cannot be ruled out. These results support the formation of a potential intramolecular disulfide bond between Cys41 and Cys46 (or between Cys41 and Cys36) in PLN monomer.

HNO-derived sulfinamides can be reduced back to free thiols in the presence of excess thiol (Keceli and Toscano, 2012). This reaction is feasible in small molecules, peptides, and proteins, but it requires hours to occur at physiological pH and temperature (Keceli and Toscano, 2012; Keceli et al., 2013), whereas under the same conditions, the reduction of disulfide bonds is typically complete within a few minutes. For instance, reverting $\sim 70\%$ of peptide sulfinamides back to reduced thiols can take up to 24 h (Keceli and Toscano, 2012). To determine how fast the reduction of HNO-derived sulfinamides is in PLN, we employed sulfinamide-modified C36,41A-PLN. In the presence of excess thiol, the timeframe of sulfinamide reduction in PLN was comparable to our previous findings obtained with short peptides (data not shown). Importantly, considering the relatively fast reversibility of HNO-induced effects observed in vitro and in vivo (Paolocci et al., 2001, 2003; Froehlich et al., 2008; Sivakumaran et al., 2013), the physiological effects of HNO on the cardiac system are likely due to the formation of disulfide linkages rather than sulfinamides.

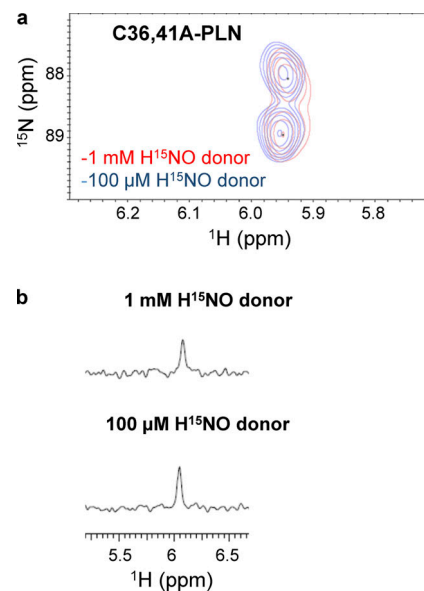


Figure 4. **Sulfinamide formation on C36,41A-PLN at different concentrations of HNO donor.** (a and b) Comparison of the sulfinamide signals generated on C36,41A-PLN (60 μ M, single Cys at position 46) upon treatment with 1 mM (red) or 100 μ M (blue) 15 N-2-MSPA by 15 N-edited 1 H 2D-NMR (a) and 15 N-edited 1 H 1D-NMR analysis (b).

HNO can target PLN cysteines 41 and 46 to increase SERCA2a activity by disrupting the SERCA2a/PLN functional interaction via sulfinamide formation

Since we determined that Cys46 and Cys41 are main targets of HNO in PLN, we next asked whether the above findings can explain the effects produced by HNO on the PLN/SERCA2a

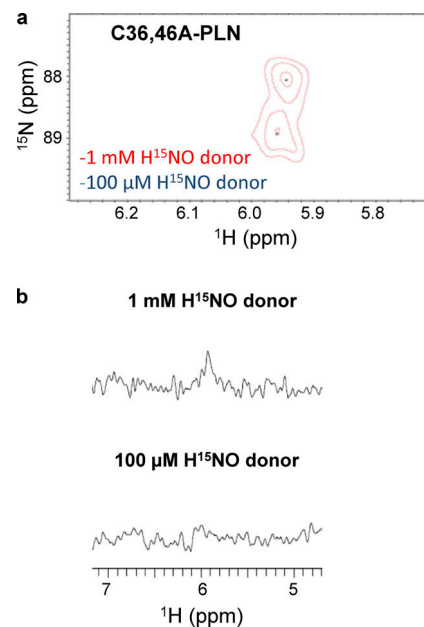


Figure 5. **Sulfinamide formation on C36,46A-PLN at different concentrations of HNO donor.** (a and b) Comparison of the sulfinamide signals generated on C36,46A-PLN (60 μ M, single Cys at position 41) upon treatment with 1 mM (red) or 100 μ M (blue) 15 N-2-MSPA by 15 N-edited 1 H 2D-NMR (a) and 15 N-edited 1 H 1D-NMR analysis (b).

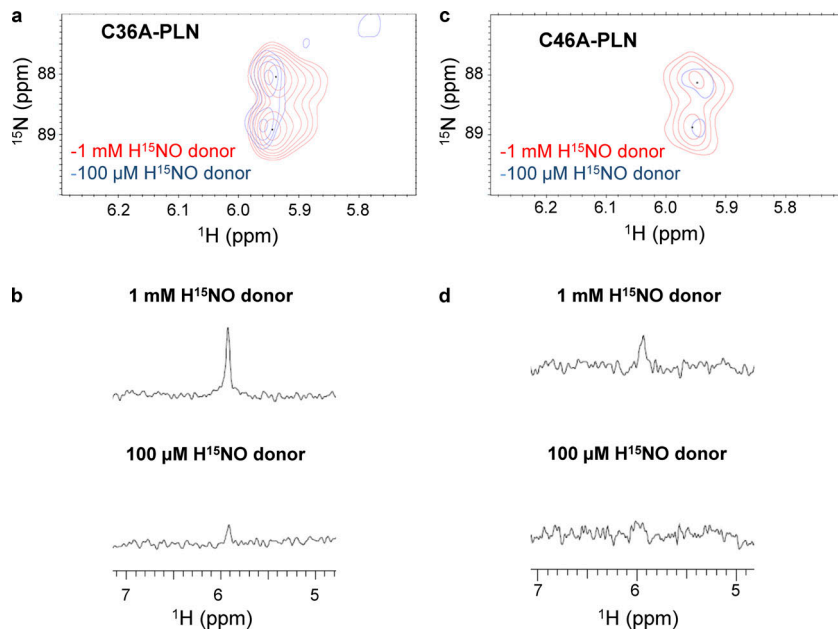


Figure 6. Sulfinamide formation on C36A-PLN at different concentrations of HNO donor. (a–d) Comparison of the sulfinamide signals generated on C36A-PLN (60 μ M, Cys at positions 41 and 46) upon treatment with 1 mM (red) or 100 μ M (blue) 15 N-2-MSPA by 15 N-edited 1 H 2D-NMR (a) and 15 N-edited 1 H 1D-NMR analysis (b). Comparison of the sulfinamide signals generated on C46A-PLN (60 μ M, Cys at positions 36 and 41) upon treatment with 1 mM (red) or 100 μ M (blue) 15 N-2-MSPA by 15 N-edited 1 H 2D-NMR (c) and 15 N-edited 1 H 1D-NMR analysis (d).

interaction, and thus SR Ca^{2+} reuptake. For this purpose, we analyzed the activity of SERCA2a coexpressed with PLN single-cysteine mutants before and after HNO treatment.

SERCA2a was under normal regulatory control of each of the individual PLN single cysteine mutants, demonstrated by the leftward shift of the $[\text{Ca}^{2+}]$ -dependent activity curve following treatment with anti-PLN monoclonal antibody, 2D12, relative to untreated samples (Fig. 7). It has been demonstrated previously that 2D12 uncouples PLN from SERCA2a, similar to PLN phosphorylation (Autry and Jones, 1997; Waggoner et al., 2004). AS/HNO treatment (100 μ M for 10 min at RT) had no significant impact on the $[\text{Ca}^{2+}]$ -dependent activity curve of SERCA2a in the presence of C41,46A-PLN, suggesting that PLN residue Cys36 is not primarily involved in the HNO-induced functional effects on the SERCA2a/PLN system. In contrast, AS/HNO shifted the $[\text{Ca}^{2+}]$ -dependent activity curve of SERCA2a in the presence of both

C36,46A-PLN and C36,41A-PLN, similar to that observed for 2D12 treatment of each sample. Our findings clearly indicate that AS/HNO modification of PLN at these residues functionally uncouples PLN from SERCA2a. Thus, in agreement with our NMR data, these SERCA2a activity data demonstrate that PLN cysteines 41 and 46 are the targets of HNO, and consequently point to the potential disruption of SERCA2a/PLN functional interaction due to the formation of a sulfinamide, which is the expected HNO-derived modification in these PLN single-cysteine mutants.

Blocking PLN cysteines with CPM prevents HNO-induced activation of SERCA2a in isolated cardiomyocytes, abating HNO ability of increasing sarcomere shortening

To determine if the impact of HNO on PLN cysteines correlates with the effects of HNO on cardiomyocytes, we analyzed the

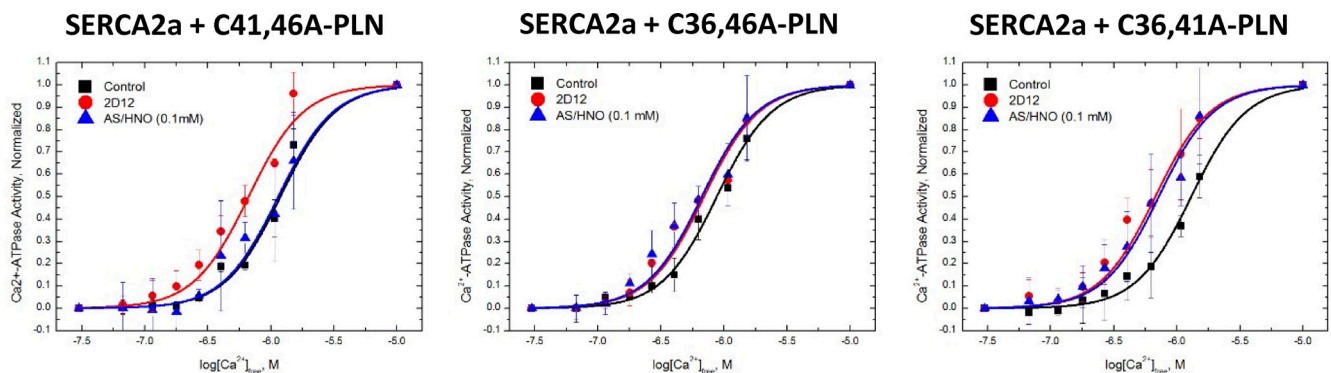


Figure 7. PLN cysteine residues 41 and 46 are important for the functional uncoupling of PLN from SERCA2a by HNO. High Five insect cell microsomes containing SERCA2a coexpressed with PLN single cysteine constructs (C41,46A-PLN [single Cys at position at 36; left], C36,46A-PLN [single Cys at position at 41; middle], C36,41A-PLN [single Cys at position at 46; right]) were suspended (0.2 mg total protein/ml) in 250 mM sucrose and 10 mM imidazole, pH 7.0, treated with either vehicle (squares), anti-PLN monoclonal antibody 2D12 (circles), or 100 μ M AS (triangles) and incubated at room temperature for 10 min, after which the treated microsomes were assayed for $[\text{Ca}^{2+}]$ -dependent ATPase activity at 37°C. The data are shown normalized to their respective maximas to better illustrate the AS/HNO-dependent shift in the $[\text{Ca}^{2+}]$ -dependent activity curve. Symbols are the average of three experiments, and the error bars represent the SD.

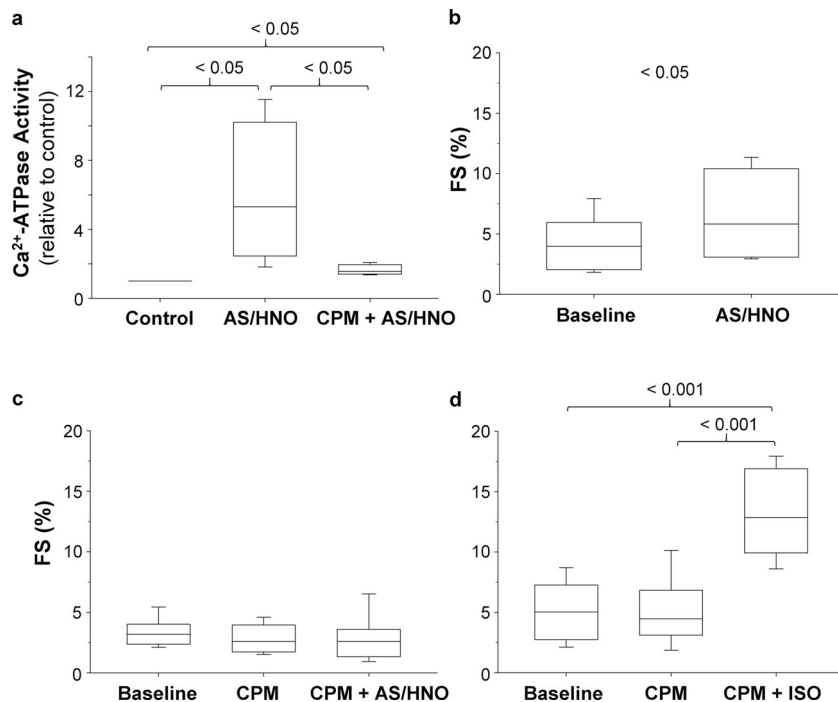


Figure 8. Blocking cysteines prevents HNO-induced SERCA2a activation and abates increase in sarcomere shortening in cardiomyocytes. (a) Cardiomyocytes resuspended in Ca²⁺-free assay buffer at pH 7.0 (0.5 mg total protein/ml), were incubated with vehicle or CPM (5 μ M) for 15 min at room temperature. Following treatment with 0 or 100 μ M AS/HNO, the samples were assayed for [Ca²⁺]-dependent ATPase activity at 1 μ M [Ca²⁺]_{free} at 37°C. The data were normalized with respect to the activity of control samples ($n = 4$; *, $P < 0.05$). (b–d) Summary data of the impact of (b) AS/HNO (500 μ M; $n = 5$ cells for each group; *, $P < 0.05$), (c) CPM (20 nM) followed by AS/HNO (500 μ M; $n = 9$ –14 cells for each group obtained from four to five different mice; $P = \text{NS}$), and (d) CPM (20 nM) followed by ISO (10 nM; $n = 10$ cells for each group obtained from four different mice; ***, $P < 0.001$ versus basal, ***, $P < 0.001$ versus CPM alone) on fractional sarcomere shortening (FS) expressed as fractional increase from diastolic levels for WT cardiomyocytes.

Ca²⁺-dependent ATPase activity. As expected, cardiomyocytes isolated from WT mouse hearts showed a significant increase in SERCA2a activity upon treatment with AS/HNO (Fig. 8 a). Importantly, the blockade of cysteines with a thiol-specific alkylating agent, CPM, abated the HNO-induced SERCA2a activation markedly, thus further validating the pivotal role exerted by cysteines in HNO-mediated acceleration of SR Ca²⁺ uptake. Likely, the residual activation could be attributed to an incomplete alkylation of PLN cysteines by CPM, presumably due to steric hindrance.

Next, we tested whether CPM is able to prevent HNO-induced enhancement of myocyte contractility. Consistent with our previous evidence (Tocchetti et al., 2007; Sivakumaran et al., 2013), HNO increased sarcomere shortening (Fig. 8 b). Of note, this effect was nearly abolished when isolated myocytes were preincubated with CPM to block cysteine residues, including those present in PLN (Fig. 8 c). As a control and in order to consolidate previous evidence attesting that HNO inotropy is different from that elicited by other agents such as β 1– β 2 agonists, a separate set of CPM-treated myocytes were superfused with the β 1– β 2 agonist, ISO (10 nM for 10 min). These cells responded in full to ISO (Fig. 8 d). Thus, this set of data validates previous evidence obtained in PLN KO mice (Sivakumaran et al., 2013), further attesting that muting PLN cysteines results in lack of HNO stimulation of isolated cardiomyocytes.

Discussion

We have provided new NMR-based evidence showing that cysteines 46 and 41 are the major sites of HNO reactivity in PLN, with cysteine 46 being most reactive. This chemical evidence is fully supported by functional studies in High Five microsomes, showing that when these two residues are mutated to alanines,

HNO-induced enhancement of SERCA2a activity is significantly reduced. Furthermore, our results indicate that sulfinamide formation is the preferred HNO-induced cysteine modification when the HNO donor is in excess with respect to thiols, whereas at ~1:1 HNO/thiol ratios (presumably more similar to normal in vivo conditions), an intramolecular disulfide bond likely dominates.

Cardiac function is regulated by varying the cytosolic Ca²⁺ ion concentration in heart muscle cells. The trigger for cardiac muscle contraction is a large ($\cong 1 \mu$ M) cytosolic concentration of Ca²⁺, and the signal for relaxation is a roughly 90% drop in the Ca²⁺ concentration. These fluctuations are achieved in part by the release and capture of Ca²⁺ ions by the SR. In humans, greater than 70% of cytosolic Ca²⁺ is pumped into the SR by SERCA2a. The luminal Ca²⁺ is released back into the cytosol by Ca²⁺-release channels (RYRs; MacLennan and Kranias, 2003). PLN is a 52-amino acid transmembrane protein that is located in the SR. PLN is associated with SERCA2a, and depending on its phosphorylation state, regulates the activity of SERCA2a (Li et al., 2003; MacLennan and Kranias, 2003; James et al., 2012). Sequence analysis of PLN has shown that the 6.1-kD protein is organized in three domains: cytosolic domain Ia (residues 1–20), cytosolic domain Ib (21–30), and domain II (31–52), which traverses the membrane (Simmerman and Jones, 1998). Domain Ia is a cytosolic helical region containing Ser16, the site of phosphorylation by PKA (James et al., 1989). Despite this cytosolic phosphorylation, studies have shown that the inhibition of SERCA2a is due to the interaction of the transmembrane region of PLN and SERCA2a (Kimura et al., 1996). Hence, it is suggested that the interaction between PLN cytosolic domain Ia and SERCA2a is not inhibitory, but phosphorylation in this domain prompts a conformational change that disrupts the inhibitory transmembrane interaction. PLN exists as an equilibrium

mixture of a monomeric and a pentameric species, which is held together by hydrophobic interactions (Wegener and Jones, 1984; Jones et al., 1985). Site-directed mutagenesis studies have shown that PLN-PLN and PLN-SERCA2a interactions are on opposite faces of the PLN transmembrane helix, and identified PLN monomer as the inhibitory species (Kimura et al., 1997). Our work involving coimmunoprecipitation, fluorescence spectroscopy, and electron paramagnetic resonance spectroscopy studies with HNO-treated SERCA/PLN complex indicates that HNO functionally uncouples PLN from SERCA, although the physical association remains (Sivakumaran et al., 2013).

In addition to phosphorylation, we and others have shown that redox-based post-translational modifications are also equally relevant in modulating the SERCA2a/PLN interaction (Bigelow and Squier, 2005; Froehlich et al., 2008; Lancel et al., 2009; Ha et al., 2011; Sivakumaran et al., 2013; Irie et al., 2015). We first reported that HNO stimulates SERCA2a Ca^{2+} uptake in a PLN-dependent manner, and that PLN cysteines are involved in these HNO-induced changes (Froehlich et al., 2008; Sivakumaran et al., 2013). Using isolated cardiomyocytes and whole hearts from WT and PLN KO mice, we showed that the HNO-induced positive inotropy/lusitropy is lost in PLN-null hearts/myocytes (Sivakumaran et al., 2013), and that HNO actions are PKA-independent, as confirmed by the lack of Ser16 phosphorylation on PLN after HNO treatment (Sivakumaran et al., 2013). In keeping with all this preceding evidence, the present findings demonstrate that preblocking cysteines prevents the increase in sarcomere shortening and SERCA2a activation due to HNO, while preserving the sensitivity of the sarcomere contractile apparatus to $\beta 1$ - $\beta 2$ agonists. Thus, as a therapeutic vector, HNO enhances myocyte Ca^{2+} cycling without relying on βAR /PKA signaling. Moreover, genetic alterations of PLN may result in an attenuation or ablation of HNO impact on Ca^{2+} cycling, a possibility that remains to be tested in full.

There is a wide palette of redox-based post-translational modifications that can affect the SERCA2a/PLN interaction on SERCA2a, PLN, or both. One possibility is that HNO sequesters amounts of monomeric, inhibitory PLN in the guise of dimers or tetramers, likely via disulfide bond formation, as demonstrated in microsomal samples, isolated cardiomyocytes, and heart extracts (Froehlich et al., 2008; Sivakumaran et al., 2013). In fact, DTT fully reverses HNO-induced PLN oligomerization (Froehlich et al., 2008; Sivakumaran et al., 2013). Similarly, the formation of disulfide bonds in a missense mutation of PLN (R9C) upon oxidation by ROS, as well as the contribution of PLN S-nitrosylation to PLN pentamerization in the process of controlling Ca^{2+} homeostasis, point to a major role exerted by redox-based mechanisms on the SERCA2a/PLN interactome (Ha et al., 2011; Irie et al., 2015). Furthermore, reversible oxidative modifications on PLN Met20 following oxidative/nitrosative stress have been proposed to result in helix destabilization of PLN, thus affecting SERCA2a activation (Ruse et al., 2004; Bigelow and Squier, 2005). Finally, modulation of pump activity due to RNS-related S-glutathiolation of SERCA2a has been reported (Adachi et al., 2004; Lancel et al., 2009).

The present results deepen our understanding of how HNO affects the SERCA2a/PLN interaction, resulting in an increased

catalytic efficiency of the SERCA2a pump. First, they identify PLN Cys41 and Cys46 as the most reactive thiols toward HNO. Furthermore, the observed relief of inhibition on SERCA2a, i.e., the functional uncoupling (structural rearrangement without physical dissociation) between the pump and PLN single cysteine mutants, presumably due to an HNO-derived sulfinamide modification, may also point to the importance of these residues on the SERCA2a/PLN interaction. In addition to potential disulfide formation in WT-PLN, our results suggest that the generation of a sulfinamide on either Cys41 or Cys46 is also capable of altering PLN regulation of SERCA2a activity. Consonant to this eventuality, recent studies using several different techniques emphasize the role of PLN conformational changes in affecting SERCA activity (James et al., 2012; Gustavsson et al., 2013; Dong and Thomas, 2014). Some of them suggest that SERCA2a activity is regulated by an equilibrium among three transient conformational states of PLN and the relief of SERCA inhibition by a shift in this equilibrium upon PLN phosphorylation (Gustavsson et al., 2013). In addition, mutation of PLN residues have been shown to influence SERCA function by affecting the interaction of SERCA/PLN complex, directly or by changing PLN structural dynamics (Kimura et al., 1998; Trieber et al., 2005; Ha et al., 2007; Glaves et al., 2011). Although further studies are required, present and previous studies suggest that HNO can induce a conformational change in SERCA-associated PLN via the formation of an intramolecular disulfide linkage and/or sulfinamide, which disturbs its functional coupling with the Ca^{2+} pump.

At a low HNO/thiol ratio, our results point to the formation of a potential intramolecular disulfide bond, whose exact characterization and location require further investigation. Our previous work suggests that HNO-induced PLN oligomerization at least partially occurs in the pentameric structure (Froehlich et al., 2008; Sivakumaran et al., 2013). A limitation of the present study is the lack of pentameric species in double-cysteine variants of PLN (C36A-PLN [Cys at positions 41 and 46] and C46A-PLN [Cys at positions 36 and 41]). In our hands, these variants migrate as a mixture of monomer and dimer on SDS-PAGE gels, thus preventing the analysis of intermolecular disulfide bond formation. Moreover, the present lack of any detectable HNO-induced modification on Cys36 could be due to nonthiol trapping of the *N*-hydroxysulfenamide intermediate and/or the formation of an unstable sulfinamide whose detection and reactivity also require future dedicated analysis.

Finally, high in vitro concentrations of HNO that may mimic excessive in vivo HNO production and signaling are expected to result in sulfinamide formation on cysteine residues, which is not readily reversible under physiologically relevant conditions (Keceli and Toscano, 2012; Keceli et al., 2013; Fukuto, 2019). Conversely, HNO-positive inotropic and lusitropic actions in vivo have been observed with low (nM range) concentrations (Paolocci et al., 2003; Tocchetti et al., 2007) and reported to be reversible (Paolocci et al., 2003; Tocchetti et al., 2007; Irvine et al., 2013; Kemp-Harper et al., 2016). Given the few viable methodologies able to detect HNO in biological systems, it is difficult to determine HNO concentrations accurately in vivo (Kemp-Harper, 2011; Doctorovich et al., 2014; Rivera-Fuentes

and Lippard, 2015). However, similar to the concentrations employed in the present and previous studies (at low HNO/thiol ratios), in vivo HNO concentrations are not expected to be in excess of PLN (Paolucci et al., 2001, 2003; Tocchetti et al., 2007, 2011; Gao et al., 2012). Moreover, the easily reversible nature of HNO-induced effects on cardiac function strongly support that disulfide formation likely dominates upon exposure of PLN to HNO in vivo. Among various RNS/ROS-induced post-translational modifications of thiols, sulfinamide formation is unique to HNO. Thus, our studies imply that HNO is able to affect the PLN/SERCA2a interaction in different, and likely complementary, ways to other RNS/ROS species. We believe that the impact of “low versus high titers of HNO,” particularly with respect to chronic (long-term) signaling, could be more definitely resolved once more accurate methods for HNO detection in vivo are available.

Conclusions

NMR analysis of sulfinamide detection along with biochemical activity studies have established that Cys46 and Cys41 are the selective targets of HNO reactivity with PLN, a conclusion further corroborated by the fact that mutation of PLN cysteine 46 or 41 to alanine reduces the HNO-induced enhancement of SERCA2a activity. HNO leads to sulfinamide formation when it is in excess with respect to thiols, but HNO induces disulfide bond formation when the HNO/thiol stoichiometry approaches a 1:1 ratio. Given that the latter condition is more likely to occur in vivo under normal physiological conditions, the present findings lend further support to previous in vivo and in vitro observations showing that HNO cardiovascular actions are easily reversible after discontinuing HNO donor infusion and/or upon administration of reducing agents such as glutathione or DTT. Moreover, the present studies demonstrate the use of ¹⁵N-edited NMR spectroscopy to detect redox changes on thiols that are unique to HNO, thus advancing our ability to detect HNO footprints in biological systems, while parsing them out from chemical modifications imparted by other RNS/ROSS. In essence, they further suggest HNO as a potential signaling molecule in the cardiovascular system.

Acknowledgments

The authors thank Dr. David A. Kass for facilitating the studies and Mr. Brandon Pfeifer for his assistance in the preparation of PLN double-cysteine variants.

This work was supported by National Science Foundation grant CHE-1566065 (to J.P. Toscano); by American Heart Association grant AHA GIA 17070027; National Institutes of Health grants NIH R01 HL136918 (to N. Paolucci), and NIH R01 HL063030 (N. Paolucci as Co-Principal Investigator); by the T32 National Institutes of Health training grant 1T32AG058527 (G. Keceli); and by the Magic-That-Matters Johns Hopkins University Funding (to N. Paolucci).

N. Paolucci and J.P. Toscano are scientific co-founders and stockholders of Cardioxyl Pharmaceuticals/BMS.

Author contributions: G. Keceli conducted most of the experiments and analyzed the results. A. Majumdar provided

technical assistance and contributed to the preparation of Figs. 2 through 6. C.N. Thorpe and J.E. Mahaney performed and analyzed the experiments shown in Fig. 7. S. Jun, C.G. Tocchetti, and D.I. Lee performed and analyzed the experiments shown in Fig. 8, b–d. G. Keceli, N. Paolucci, and J.P. Toscano wrote the paper. J.E. Mahaney, N. Paolucci, and J.P. Toscano conceived the idea for the project. All authors reviewed the results and approved the final version of the manuscript.

Henk L. Granzier served as editor.

Submitted: 7 August 2018

Accepted: 15 February 2019

References

- Abu-Baker, S., and G.A. Lorigan. 2006. Phospholamban and its phosphorylated form interact differently with lipid bilayers: a ³¹P, ²H, and ¹³C solid-state NMR spectroscopic study. *Biochemistry*. 45:13312–13322. <https://doi.org/10.1021/bi0614028>
- Adachi, T., R.M. Weisbrod, D.R. Pimentel, J. Ying, V.S. Sharov, C. Schöneich, and R.A. Cohen. 2004. S-Glutathiolation by peroxynitrite activates SERCA during arterial relaxation by nitric oxide. *Nat. Med.* 10:1200–1207. <https://doi.org/10.1038/nm1119>
- Autry, J.M., and L.R. Jones. 1997. Functional Co-expression of the canine cardiac Ca²⁺ pump and phospholamban in *Spodoptera frugiperda* (Sf21) cells reveals new insights on ATPase regulation. *J. Biol. Chem.* 272:15872–15880. <https://doi.org/10.1074/jbc.272.25.15872>
- Bachi, A., I. Dalle-Donne, and A. Scaloni. 2013. Redox proteomics: chemical principles, methodological approaches and biological/biomedical promises. *Chem. Rev.* 113:596–698. <https://doi.org/10.1021/cr300073p>
- Bers, D.M. 2002. Cardiac excitation-contraction coupling. *Nature*. 415:198–205. <https://doi.org/10.1038/415198a>
- Bigelow, D.J., and T.C. Squier. 2005. Redox modulation of cellular signaling and metabolism through reversible oxidation of methionine sensors in calcium regulatory proteins. *Biochim. Biophys. Acta*. 1703:121–134. <https://doi.org/10.1016/j.bbapap.2004.09.012>
- Bonner, F.T., and B. Ravid. 1975. Thermal decomposition of oxyhyponitrite (sodium trioxodinitrate(ii)) in aqueous solution. *Inorg. Chem.* 14:558–563. <https://doi.org/10.1021/ic50145a022>
- Breeze, A.L. 2000. Isotope-filtered NMR methods for the study of biomolecular structure and interactions. *Prog. Nucl. Magn. Reson. Spectrosc.* 36:323–372. [https://doi.org/10.1016/S0079-6565\(00\)00020-0](https://doi.org/10.1016/S0079-6565(00)00020-0)
- Doctorovich, F., D.E. Bikiel, J. Pellegrino, S.A. Suarez, and M.A. Marti. 2014. How to find an HNO needle in a (bio)-chemical haystack. *Prog. Inorg. Chem.* 58:145–183.
- Dong, X., and D.D. Thomas. 2014. Time-resolved FRET reveals the structural mechanism of SERCA-PLB regulation. *Biochem. Biophys. Res. Commun.* 449:196–201. <https://doi.org/10.1016/j.bbrc.2014.04.166>
- Donzelli, S., M.G. Espey, D.D. Thomas, D. Mancardi, C.G. Tocchetti, L.A. Ridnour, N. Paolucci, S.B. King, K.M. Miranda, G. Lazzarino, et al. 2006. Discriminating formation of HNO from other reactive nitrogen oxide species. *Free Radic. Biol. Med.* 40:1056–1066. <https://doi.org/10.1016/j.freeradbiomed.2005.10.058>
- Doyle, M.P., S.N. Mahapatro, R.D. Broene, and J.K. Guy. 1988. Oxidation and reduction of hemoproteins by trioxodinitrate(ii). The role of nitrosyl hydride and nitrite. *J. Am. Chem. Soc.* 110:593–599. <https://doi.org/10.1021/ja00210a047>
- Feilisch, M. 2003. Nitroxyl gets to the heart of the matter. *Proc. Natl. Acad. Sci. USA*. 100:4978–4980. <https://doi.org/10.1073/pnas.1031571100>
- Feng, W., G. Liu, R. Xia, J.J. Abramson, and I.N. Pessah. 1999. Site-selective modification of hyperreactive cysteines of ryanodine receptor complex by quinones. *Mol. Pharmacol.* 55:821–831.
- Froehlich, J.P., J.E. Mahaney, G. Keceli, C.M. Pavlos, R. Goldstein, A.J. Redwood, C. Sumbilla, D.I. Lee, C.G. Tocchetti, D.A. Kass, et al. 2008. Phospholamban thiols play a central role in activation of the cardiac muscle sarcoplasmic reticulum calcium pump by nitroxyl. *Biochemistry*. 47:13150–13152. <https://doi.org/10.1021/bi801925p>
- Fujii, J., A. Ueno, K. Kitano, S. Tanaka, M. Kadoma, and M. Tada. 1987. Complete complementary DNA-derived amino acid sequence of canine cardiac phospholamban. *J. Clin. Invest.* 79:301–304. <https://doi.org/10.1172/JCI112799>

- Fujii, J., K. Maruyama, M. Tada, and D.H. MacLennan. 1989. Expression and site-specific mutagenesis of phospholamban. Studies of residues involved in the phosphorylation and pentamer formation. *J. Biol. Chem.* 264: 12950–12955.
- Fukuto, J.M. 2019. A recent history of nitroxyl chemistry, pharmacology and therapeutic potential. *Br. J. Pharmacol.* 176:135–146. <https://doi.org/10.1111/bph.14384>
- Gao, W.D., C.I. Murray, Y. Tian, X. Zhong, J.F. DuMond, X. Shen, B.A. Stanley, D.B. Foster, D.A. Wink, S.B. King, et al. 2012. Nitroxyl-mediated disulfide bond formation between cardiac myofilament cysteines enhances contractile function. *Circ. Res.* 111:1002–1011. <https://doi.org/10.1161/CIRCRESAHA.112.270827>
- Glaves, J.P., C.A. Trieber, D.K. Ceholski, D.L. Stokes, and H.S. Young. 2011. Phosphorylation and mutation of phospholamban alter physical interactions with the sarcoplasmic reticulum calcium pump. *J. Mol. Biol.* 405: 707–723. <https://doi.org/10.1016/j.jmb.2010.11.014>
- Gustavsson, M., R. Verardi, D.G. Mullen, K.R. Mote, N.J. Traaseth, T. Gopinath, and G. Veglia. 2013. Allosteric regulation of SERCA by phosphorylation-mediated conformational shift of phospholamban. *Proc. Natl. Acad. Sci. USA.* 110:17338–17343. <https://doi.org/10.1073/pnas.1303006110>
- Ha, K.N., N.J. Traaseth, R. Verardi, J. Zamoan, A. Cembran, C.B. Karim, D.D. Thomas, and G. Veglia. 2007. Controlling the inhibition of the sarcoplasmic Ca^{2+} -ATPase by tuning phospholamban structural dynamics. *J. Biol. Chem.* 282:37205–37214. <https://doi.org/10.1074/jbc.M704056200>
- Ha, K.N., L.R. Masterson, Z. Hou, R. Verardi, N. Walsh, G. Veglia, and S.L. Robia. 2011. Lethal Arg9Cys phospholamban mutation hinders Ca^{2+} -ATPase regulation and phosphorylation by protein kinase A. *Proc. Natl. Acad. Sci. USA.* 108:2735–2740. <https://doi.org/10.1073/pnas.1013987108>
- Hagemann, D., and R.-P. Xiao. 2002. Dual site phospholamban phosphorylation and its physiological relevance in the heart. *Trends Cardiovasc. Med.* 12:51–56. [https://doi.org/10.1016/S1050-1738\(01\)00145-1](https://doi.org/10.1016/S1050-1738(01)00145-1)
- Hoffman, M.D., G.M. Walsh, J.C. Rogalski, and J. Kast. 2009. Identification of nitroxyl-induced modifications in human platelet proteins using a novel mass spectrometric detection method. *Mol. Cell. Proteomics.* 8: 887–903. <https://doi.org/10.1074/mcp.M800230-MCP200>
- Hughes, M.N., and R. Cammack. 1999. Synthesis, chemistry, and applications of nitroxyl ion releasers sodium trioxodinitrate or Angeli's salt and Piloty's acid. *Methods Enzymol.* 301:279–287. [https://doi.org/10.1016/S0076-6879\(99\)01092-7](https://doi.org/10.1016/S0076-6879(99)01092-7)
- Irie, T., P.Y. Sips, S. Kai, K. Kida, K. Ikeda, S. Hirai, K. Moazzami, P. Jiramongkolchai, D.B. Bloch, P.-T. Doulias, et al. 2015. S-nitrosylation of calcium-handling proteins in cardiac adrenergic signaling and hypertrophy. *Circ. Res.* 117:793–803. <https://doi.org/10.1161/CIRCRESAHA.115.307157>
- Irvine, J.C., R.M. Ravi, B.K. Kemp-Harper, and R.E. Widdop. 2013. Nitroxyl donors retain their depressor effects in hypertension. *Am. J. Physiol. Heart Circ. Physiol.* 305:H939–H945. <https://doi.org/10.1152/ajpheart.00630.2012>
- James, P., M. Inui, M. Tada, M. Chiesi, and E. Carafoli. 1989. Nature and site of phospholamban regulation of the Ca^{2+} pump of sarcoplasmic reticulum. *Nature.* 342:90–92. <https://doi.org/10.1038/342090a0>
- James, Z.M., J.E. McCaffrey, K.D. Torgersen, C.B. Karim, and D.D. Thomas. 2012. Protein-protein interactions in calcium transport regulation probed by saturation transfer electron paramagnetic resonance. *Biophys. J.* 103:1370–1378. <https://doi.org/10.1016/j.bpj.2012.08.032>
- Jones, L.R., H.K.B. Simmerman, W.W. Wilson, F.R.N. Gurd, and A.D. Wegener. 1985. Purification and characterization of phospholamban from canine cardiac sarcoplasmic reticulum. *J. Biol. Chem.* 260:7721–7730.
- Karim, C.B., J.D. Stamm, J. Karim, L.R. Jones, and D.D. Thomas. 1998. Cysteine reactivity and oligomeric structures of phospholamban and its mutants. *Biochemistry.* 37:12074–12081. <https://doi.org/10.1021/bi980642n>
- Karim, C.B., C.G. Marquardt, J.D. Stamm, G. Barany, and D.D. Thomas. 2000. Synthetic null-cysteine phospholamban analogue and the corresponding transmembrane domain inhibit the Ca -ATPase. *Biochemistry.* 39: 10892–10897. <https://doi.org/10.1021/bi0003543>
- Keceli, G., and J.P. Toscano. 2012. Reactivity of nitroxyl-derived sulfonamides. *Biochemistry.* 51:4206–4216. <https://doi.org/10.1021/bi300015u>
- Keceli, G., and J.P. Toscano. 2014. Reactivity of C-terminal cysteines with HNO. *Biochemistry.* 53:3689–3698. <https://doi.org/10.1021/bi500360x>
- Keceli, G., C.D. Moore, J.W. Labonte, and J.P. Toscano. 2013. NMR detection and study of hydrolysis of HNO-derived sulfonamides. *Biochemistry.* 52: 7387–7396. <https://doi.org/10.1021/bi401110f>
- Kemp-Harper, B.K. 2011. Nitroxyl (HNO): a novel redox signaling molecule. *Antioxid. Redox Signal.* 14:1609–1613. <https://doi.org/10.1089/ars.2011.3937>
- Kemp-Harper, B.K., J.D. Horowitz, and R.H. Ritchie. 2016. Therapeutic potential of nitroxyl (HNO) donors in the management of acute decompensated heart failure. *Drugs.* 76:1337–1348. <https://doi.org/10.1007/s40265-016-0631-y>
- Kimura, Y., K. Kurzydowski, M. Tada, and D.H. MacLennan. 1996. Phospholamban regulates the Ca^{2+} -ATPase through intramembrane interactions. *J. Biol. Chem.* 271:21726–21731. <https://doi.org/10.1074/jbc.271.36.21726>
- Kimura, Y., K. Kurzydowski, M. Tada, and D.H. MacLennan. 1997. Phospholamban inhibitory function is activated by depolymerization. *J. Biol. Chem.* 272:15061–15064. <https://doi.org/10.1074/jbc.272.24.15061>
- Kimura, Y., M. Asahi, K. Kurzydowski, M. Tada, and D.H. MacLennan. 1998. Phospholamban domain Ib mutations influence functional interactions with the Ca^{2+} -ATPase isoform of cardiac sarcoplasmic reticulum. *J. Biol. Chem.* 273:14238–14241. <https://doi.org/10.1074/jbc.273.23.14238>
- Laemmli, U.K. 1970. Cleavage of structural proteins during the assembly of the head of bacteriophage T4. *Nature.* 227:680–685. <https://doi.org/10.1038/227680a0>
- Lamberth, S., H. Schmid, M. Muenchbach, T. Vorherr, J. Krebs, E. Carafoli, and C. Griesinger. 2000. NMR solution structure of phospholamban. *Helv. Chim. Acta.* 83:2141–2152. [https://doi.org/10.1002/1522-2675\(20000906\)83:9<2141::AID-HLCA2141>3.0.CO;2-W](https://doi.org/10.1002/1522-2675(20000906)83:9<2141::AID-HLCA2141>3.0.CO;2-W)
- Lancel, S., J. Zhang, A. Evangelista, M.P. Trucillo, X. Tong, D.A. Siwik, R.A. Cohen, and W.S. Colucci. 2009. Nitroxyl activates SERCA in cardiac myocytes via glutathiolation of cysteine 674. *Circ. Res.* 104:720–723. <https://doi.org/10.1161/CIRCRESAHA.108.188441>
- Lanzetta, P.A., L.J. Alvarez, P.S. Reinach, and O.A. Candia. 1979. An improved assay for nanomole amounts of inorganic phosphate. *Anal. Biochem.* 100: 95–97. [https://doi.org/10.1016/0003-2697\(79\)90115-5](https://doi.org/10.1016/0003-2697(79)90115-5)
- Li, J., D.J. Bigelow, and T.C. Squier. 2003. Phosphorylation by cAMP-dependent protein kinase modulates the structural coupling between the transmembrane and cytosolic domains of phospholamban. *Biochemistry.* 42:10674–10682. <https://doi.org/10.1021/bi034708c>
- Liu, G., and I.N. Pessah. 1994. Molecular interaction between ryanodine receptor and glycoprotein triadin involves redox cycling of functionally important hyperreactive thiols. *J. Biol. Chem.* 269: 33028–33034.
- Lockwood, N.A., R.S. Tu, Z. Zhang, M.V. Tirrell, D.D. Thomas, and C.B. Karim. 2003. Structure and function of integral membrane protein domains resolved by peptide-amphiphiles: application to phospholamban. *Biopolymers.* 69:283–292. <https://doi.org/10.1002/bip.10365>
- MacLennan, D.H., and E.G. Kranias. 2003. Phospholamban: a crucial regulator of cardiac contractility. *Nat. Rev. Mol. Cell Biol.* 4:566–577. <https://doi.org/10.1038/nrml151>
- Oxenoid, K., and J.J. Chou. 2005. The structure of phospholamban pentamer reveals a channel-like architecture in membranes. *Proc. Natl. Acad. Sci. USA.* 102:10870–10875. <https://doi.org/10.1073/pnas.0504920102>
- Paolucci, N., W.F. Saavedra, K.M. Miranda, C. Martignani, T. Isoda, J.M. Hare, M.G. Espey, J.M. Fukuto, M. Feelisch, D.A. Wink, and D.A. Kass. 2001. Nitroxyl anion exerts redox-sensitive positive cardiac inotropy in vivo by calcitonin gene-related peptide signaling. *Proc. Natl. Acad. Sci. USA.* 98:10463–10468. <https://doi.org/10.1073/pnas.181191198>
- Paolucci, N., T. Katori, H.C. Champion, M.E. St. John, K.M. Miranda, J.M. Fukuto, D.A. Wink, and D.A. Kass. 2003. Positive inotropic and lusitropic effects of HNO/NO⁻ in failing hearts: independence from beta-adrenergic signaling. *Proc. Natl. Acad. Sci. USA.* 100:5537–5542. <https://doi.org/10.1073/pnas.0937302100>
- Paolucci, N., M.I. Jackson, B.E. Lopez, K. Miranda, C.G. Tocchetti, D.A. Wink, A.J. Hobbs, and J.M. Fukuto. 2007. The pharmacology of nitroxyl (HNO) and its therapeutic potential: not just the Janus face of NO. *Pharmacol. Ther.* 113:442–458. <https://doi.org/10.1016/j.pharmthera.2006.11.002>
- Rivera-Fuentes, P., and S.J. Lippard. 2015. Metal-based optical probes for live cell imaging of nitroxyl (HNO). *Acc. Chem. Res.* 48:2927–2934. <https://doi.org/10.1021/acs.accounts.5b00388>
- Ruse, C.I., F.-L. Tan, M. Kinter, and M. Bond. 2004. Integrated analysis of the human cardiac transcriptome, proteome and phosphoproteome. *Proteomics.* 4:1505–1516. <https://doi.org/10.1002/pmic.200300682>
- Sabbah, H.N., C.G. Tocchetti, M. Wang, S. Daya, R.C. Gupta, R.S. Tunin, R. Mazhari, E. Takimoto, N. Paolucci, D. Cowart, et al. 2013. Nitroxyl (HNO): A novel approach for the acute treatment of heart failure. *Circ Heart Fail.* 6:1250–1258. <https://doi.org/10.1161/CIRCHEARTFAILURE.113.000632>

- Simmerman, H.K.B., and L.R. Jones. 1998. Phospholamban: protein structure, mechanism of action, and role in cardiac function. *Physiol. Rev.* 78: 921–947. <https://doi.org/10.1152/physrev.1998.78.4.921>
- Simmerman, H.K.B., J.H. Collins, J.L. Theibert, A.D. Wegener, and L.R. Jones. 1986. Sequence analysis of phospholamban. Identification of phosphorylation sites and two major structural domains. *J. Biol. Chem.* 261:13333–13341.
- Sivakumaran, V., B.A. Stanley, C.G. Tocchetti, J.D. Ballin, V. Caceres, L. Zhou, G. Keceli, P.P. Rainer, D.I. Lee, S. Huke, et al. 2013. HNO enhances SERCA2a activity and cardiomyocyte function by promoting redox-dependent phospholamban oligomerization. *Antioxid. Redox Signal.* 19: 1185–1197. <https://doi.org/10.1089/ars.2012.5057>
- Smeazzetto, S., A. Saponaro, H.S. Young, M.R. Moncelli, and G. Thiel. 2013. Structure-function relation of phospholamban: modulation of channel activity as a potential regulator of SERCA activity. *PLoS One.* 8:e52744. <https://doi.org/10.1371/journal.pone.0052744>
- Smith, P.K., R.I. Krohn, G.T. Hermanson, A.K. Mallia, F.H. Gartner, M.D. Provenzano, E.K. Fujimoto, N.M. Goeke, B.J. Olson, and D.C. Klenk. 1985. Measurement of protein using bicinchoninic acid. *Anal. Biochem.* 150:76–85. [https://doi.org/10.1016/0003-2697\(85\)90442-7](https://doi.org/10.1016/0003-2697(85)90442-7)
- Stokes, D.L., A.J. Pomfret, W.J. Rice, J.P. Graves, and H.S. Young. 2006. Interactions between Ca^{2+} -ATPase and the pentameric form of phospholamban in two-dimensional co-crystals. *Biophys. J.* 90:4213–4223. <https://doi.org/10.1529/biophysj.105.079640>
- Tocchetti, C.G., W. Wang, J.P. Froehlich, S. Huke, M.A. Aon, G.M. Wilson, G. Di Benedetto, B. O'Rourke, W.D. Gao, D.A. Wink, et al. 2007. Nitroxyl improves cellular heart function by directly enhancing cardiac sarcoplasmic reticulum Ca^{2+} cycling. *Circ. Res.* 100:96–104. <https://doi.org/10.1161/01.RES.0000253904.53601.c9>
- Tocchetti, C.G., B.A. Stanley, C.I. Murray, V. Sivakumaran, S. Donzelli, D. Mancardi, P. Pagliaro, W.D. Gao, J. van Eyk, D.A. Kass, et al. 2011. Playing with cardiac “redox switches”: the “HNO way” to modulate cardiac function. *Antioxid. Redox Signal.* 14:1687–1698. <https://doi.org/10.1089/ars.2010.3859>
- Toscano, J.P., F.A. Brookfield, A.D. Cohen, S.M. Courtney, L.M. Frost, and V.J. Kalish. 2011. N-hydroxylsulfonamide derivatives as new physiologically useful nitroxyl donors. US patent 8,030,356, filed March 16, 2007, and issued October 4, 2011.
- Traaseth, N.J., K.N. Ha, R. Verardi, L. Shi, J.J. Buffy, L.R. Masterson, and G. Veglia. 2008. Structural and dynamic basis of phospholamban and sarcoplasmic inhibition of Ca^{2+} -ATPase. *Biochemistry.* 47:3–13. <https://doi.org/10.1021/bi701668v>
- Traaseth, N.J., L. Shi, R. Verardi, D.G. Mullen, G. Barany, and G. Veglia. 2009. Structure and topology of monomeric phospholamban in lipid membranes determined by a hybrid solution and solid-state NMR approach. *Proc. Natl. Acad. Sci. USA.* 106:10165–10170. <https://doi.org/10.1073/pnas.0904290106>
- Trieber, C.A., J.L. Douglas, M. Afara, and H.S. Young. 2005. The effects of mutation on the regulatory properties of phospholamban in co-reconstituted membranes. *Biochemistry.* 44:3289–3297. <https://doi.org/10.1021/bi047878d>
- Veglia, G., K.N. Ha, L. Shi, R. Verardi, and N.J. Traaseth. 2010. What can we learn from a small regulatory membrane protein? *Methods Mol. Biol.* 654:303–319. https://doi.org/10.1007/978-1-60761-762-4_16
- Verardi, R., L. Shi, N.J. Traaseth, N. Walsh, and G. Veglia. 2011. Structural topology of phospholamban pentamer in lipid bilayers by a hybrid solution and solid-state NMR method. *Proc. Natl. Acad. Sci. USA.* 108: 9101–9106. <https://doi.org/10.1073/pnas.1016535108>
- Vostrikov, V.V., K.R. Mote, R. Verardi, and G. Veglia. 2013. Structural dynamics and topology of phosphorylated phospholamban homopentamer reveal its role in the regulation of calcium transport. *Structure.* 21: 2119–2130. <https://doi.org/10.1016/j.str.2013.09.008>
- Waggoner, J.R., J. Huffman, B.N. Griffith, L.R. Jones, and J.E. Mahaney. 2004. Improved expression and characterization of Ca^{2+} -ATPase and phospholamban in High-Five cells. *Protein Expr. Purif.* 34:56–67. <https://doi.org/10.1016/j.pep.2003.11.005>
- Wegener, A.D., and L.R. Jones. 1984. Phosphorylation-induced mobility shift in phospholamban in sodium dodecyl sulfate-polyacrylamide gels. Evidence for a protein structure consisting of multiple identical phosphorylatable subunits. *J. Biol. Chem.* 259:1834–1841.
- Wong, P.S.Y., J. Hyun, J.M. Fukuto, F.N. Shirota, E.G. DeMaster, D.W. Shoeman, and H.T. Nagasawa. 1998. Reaction between S-nitrosothiols and thiols: generation of nitroxyl (HNO) and subsequent chemistry. *Biochemistry.* 37:5362–5371. <https://doi.org/10.1021/bi973153g>
- Wouters, M.A., R.A. George, and N.L. Haworth. 2007. “Forbidden” disulfides: their role as redox switches. *Curr. Protein Pept. Sci.* 8:484–495. <https://doi.org/10.2174/138920307782411464>
- Wouters, M.A., S.W. Fan, and N.L. Haworth. 2010. Disulfides as redox switches: from molecular mechanisms to functional significance. *Antioxid. Redox Signal.* 12:53–91. <https://doi.org/10.1089/ars.2009.2510>
- Zamoon, J., A. Mascioni, D.D. Thomas, and G. Veglia. 2003. NMR solution structure and topological orientation of monomeric phospholamban in dodecylphosphocholine micelles. *Biophys. J.* 85:2589–2598. [https://doi.org/10.1016/S0006-3495\(03\)74681-5](https://doi.org/10.1016/S0006-3495(03)74681-5)
- Zhu, G., D. Groneberg, G. Sikka, D. Hori, M.J. Ranek, T. Nakamura, E. Takimoto, N. Paolucci, D.E. Berkowitz, A. Friebe, and D.A. Kass. 2015. Soluble guanylate cyclase is required for systemic vasodilation but not positive inotropy induced by nitroxyl in the mouse. *Hypertension.* 65: 385–392. <https://doi.org/10.1161/HYPERTENSIONAHA.114.04285>